Compact electro-absorption modulator integrated with vertical-cavity surface-emitting laser for highly efficient millimeter-wave modulation

Hamed Dalir, Moustafa Ahmed, Ahmed Bakry, and Fumio Koyama

Citation: Applied Physics Letters **105**, 081113 (2014); doi: 10.1063/1.4894716
View online: http://dx.doi.org/10.1063/1.4894716
View Table of Contents: http://scitation.aip.org/content/aip/journal/apl/105/8?ver=pdfcov
Published by the AIP Publishing

Compact electro-absorption modulator integrated with vertical-cavity surface-emitting laser for highly efficient millimeter-wave modulation

Hamed Dalir,[1,a)] Moustafa Ahmed,[2] Ahmed Bakry,[2] and Fumio Koyama[1,2]
[1]*Precision and Intelligence Laboratory, Photonics Integration System Research Center, Tokyo Institute of Technology, 4259-R2-22 Nagatsuta-cho, Midori-ku, Yokohama, 226-8503, Japan*
[2]*Department of Physics, Faculty of Science, King Abdulaziz University, 80203 Jeddah 21589, Saudi Arabia*

(Received 29 July 2014; accepted 21 August 2014; published online 29 August 2014)

We demonstrate a compact electro-absorption slow-light modulator laterally-integrated with an 850 nm vertical-cavity surface-emitting laser (VCSEL), which enables highly efficient millimeter-wave modulation. We found a strong leaky travelling wave in the lateral direction between the two cavities via widening the waveguide width with a taper shape. The small signal response of the fabricated device shows a large enhancement of over 55 dB in the modulation amplitude at frequencies beyond 35 GHz; thanks to the photon-photon resonance. A large group index of over 150 in a Bragg reflector waveguide enables the resonance at millimeter wave frequencies for 25 μm long compact modulator. Based on the modeling, we expect a resonant modulation at a higher frequency of 70 GHz. The resonant modulation in a compact slow-light modulator plays a significant key role for high efficient narrow-band modulation in the millimeter wave range far beyond the intrinsic modulation bandwidth of VCSELs. © *2014 AIP Publishing LLC*. [http://dx.doi.org/10.1063/1.4894716]

Wireless coverage of the end-user domain has become a key part of the broadband communication networks. In order to meet the demands of internet traffic and to prevent from the capacity crunch, wireless systems are needed to have operations at higher data rates. Radio over Fiber (RoF) defines to a technique whereby light is modulated with a radio signal and transmitted over an optical fiber link to realize the wireless connection. RoF has attracted considerable attention for the broadband wireless services.[1–5] On the contrary, millimeter-waves RoF offers considerably broad bandwidth for the ultra-fast wireless communications. However, the generation of millimeter wave signals still remains as an obstacle. The simplest method for optically distributing radio-frequency (RF) signals is the modulation of semiconductor lasers with RF signals. In this regard, a main challenge is to realize high-speed lasers in the millimeter wave range. The modulation bandwidth of semiconductor lasers is restricted by the intrinsic limitation of relaxation oscillations as well as parasitics, and is practically limited below 20 GHz. The resonant modulation of semiconductor lasers with optical feedback is an alternative for high-frequency modulations.[6–9] However, an external cavity approach needs bulk optics or hybrid integration techniques, which may suffer from excessive losses and poor stability of operations. While a resonant modulation over 20 GHz was demonstrated using a monolithically integrated passive extended cavity, a low-loss, long passive waveguide is needed.[10,11]

On the other hand, vertical-cavity surface-emitting lasers (VCSELs) have been developed for short reach optical interconnects.[12,13] The merits of VCSELs include low power consumption, small footprint, wafer-scale testing, low-cost packaging, and ease of fabrication into arrays. In addition, VCSELs offer low cost solutions for indoor applications. High-speed GaAs-based VCSELs at the wavelength range of 850–1060 nm have been developed, which offer a 3-dB modulation bandwidth over 20 GHz.[14–18] Various concepts to boost the speed of VCSELs have been explored, including injection locking,[19,20] coupled cavity,[21] and modulator-integration.[22] An interesting approach is the locking of transverse-modes either in multi-mode VCSELs or coupled-cavity VCSELs for ultra-high frequency modulation.[23–25] We have been studying optical feedback with the aim of enhancing the modulation bandwidth of VCSELs.[26–28] Also, we recently demonstrated an ultra-compact (8 μm long) electro-absorption modulator laterally integrated with a 980 nm InGaAs VCSEL incorporating a bow-tie-shaped oxide aperture.[29] A large signal modulation up to 25 Gbit/s with a low modulation voltage of 400 mV_{pp} was successfully demonstrated. Slowing light in the Bragg reflector waveguide enables us to reduce the length of a modulator and hence to increase the modulation bandwidth.[30]

In this paper, a compact electro-absorption slow-light modulator is laterally-integrated with an 850 nm VCSEL for highly efficient resonant modulations. We obtained a large enhancement of over 55 dB in the modulation amplitude at a frequency beyond 35 GHz; thanks to the resonance in the modulator. Slowing light in a Bragg reflector waveguide enables the resonance at millimeter wave frequencies for a 25 μm long ultra-compact modulator, which could reduce the parasitic capacitance for high frequency modulations. The observed resonant modulation has a significant impact for high efficient narrow-band modulation in the millimeter wave frequency, which is far beyond the intrinsic modulation bandwidth of VCSELs.

The scheme of the slow-light modulator-integrated VCSEL is shown in Fig. 1(a). The vertical structure is the same as that of conventional 850 nm VCSELs. The bottom mirror consists of a 35-period Si-doped $Al_{0.9}Ga_{0.1}As/Al_{0.15}Ga_{0.85}As$

a)dalir.h.ac@m.titech.ac.jp

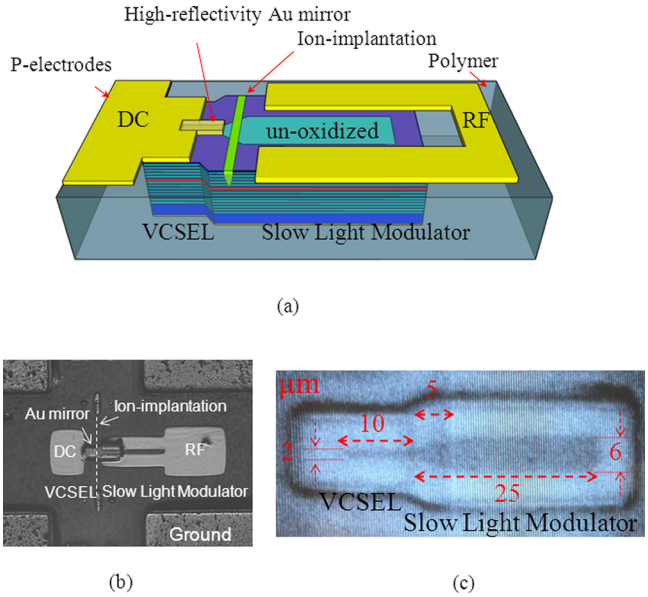

FIG. 1. (a) Schematic structure, (b) Top view, and (c) Infrared image of oxidation formation of the slow-light modulator laterally integrated with VCSEL.

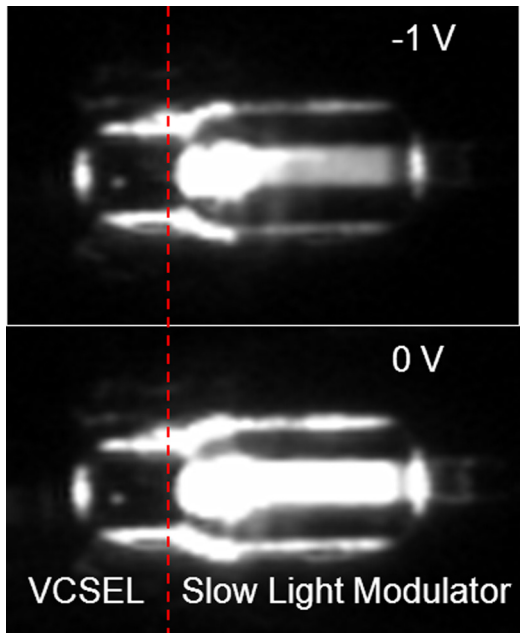

FIG. 2. The near-field patterns for different modulator voltages (un-changed intensity in the slow light waveguide is in the proton implanted region).

distributed Bragg-reflector (DBR). The active region has three $Al_{0.3}Ga_{0.7}As/GaAs$ quantum wells sandwiched in one-λ cavity. The top mirror consists of a 22.5-period carbon-doped $Al_{0.9}Ga_{0.1}As/Al_{0.15}Ga_{0.85}As$ DBR. Lateral optical confinement is formed by applying an oxide layer, while widening the waveguide width with a taper shape guides a strong leaky travelling wave in the lateral direction from the VCSEL into an electro-absorption modulator. Also, the three dimensional model of widening the oxide aperture shows that the joint section causes a reflection of several %, which forms the transverse modes in the VCSEL. The oxidation at the end of the modulator section functions as a perfect mirror, thus we are able to form the resonance in the modulator section.[27,28] A large group index of 150 in a Bragg reflector waveguide enables us to obtain the resonance at 35 GHz even for a 25 μm long compact modulator for an example, which gives us a low parasitic capacitance to increase the modulation speed. Please note that a 1 mm-long cavity is needed in conventional in-plane resonators for getting the same resonant frequency.

Figure 1(b) shows the top view of the fabricated device. Taper shaped mesas are planarized using polymer (ALX-2010, Asahi Glass), and Ground-Signal-Ground (GSG) electrodes are formed on the surface. Proton implantation with six-step different acceleration voltages from 60 to 350 kV and doses of $10^{15}\,cm^{-2}$ was performed at the center of the joint connection of the coupled cavities. According to the measured depth profile, the protons penetrated almost the entire top DBR, with the thickness of 4 μm. The electrical isolation between the two electrodes was over 10 MΩ. The infrared image of the oxide aperture is shown in Fig. 1(c). The waveguide (oxide aperture) widths of the VCSEL and the modulator are 2 μm and 6 μm, respectively. The lengths of the VCSEL and modulator sections are 10 μm and 25 μm, respectively.

Figure 2 illustrates the near field pattern for the on and off states by applying reverse bias of 0 and 1 V in the modulator side, respectively. The intensity at the modulator section clearly decreases due to the electro-absorption in QWs by applying a reverse-bias voltage. While the top emission of the VCSEL is inhibited by plating the gold on the top, the output from the modulator is obtained by collecting the power through a multi-mode fiber. Figure 3 indicates the coupled light output/current characteristics for different modulator voltages. These results show the intensity modulation results mainly from the electro-absorption. The ripples in the light-output characteristics are due to the resonance in the modulator section. We obtained a static extinction ratio of 10 dB for a reverse-bias voltage of 1 V at a VCSEL current of 8 mA. Such a low voltage could be attained even for a compact (25 μm long) modulator; thanks to a large group index of over 150 in the Bragg reflector waveguide and the resonance in the modulator section. The intensity modulation dominantly takes place in the modulator section since the intensity of the implantation region at the center is almost unchanged as shown in Fig. 2. A fiber coupled power from the modulator is −7.4 dBm at a bias current of 8 mA, which

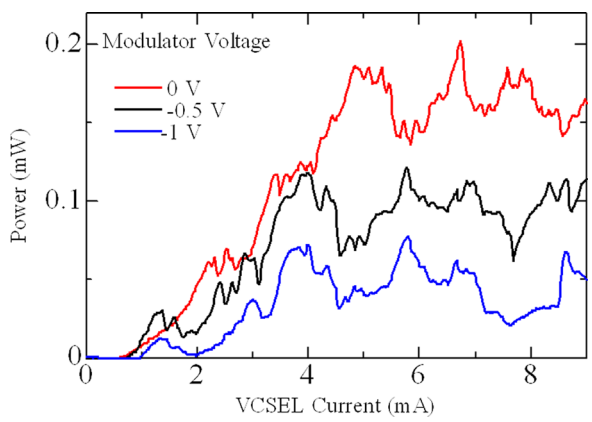

FIG. 3. Coupled light output/current characteristics for different modulator voltages.

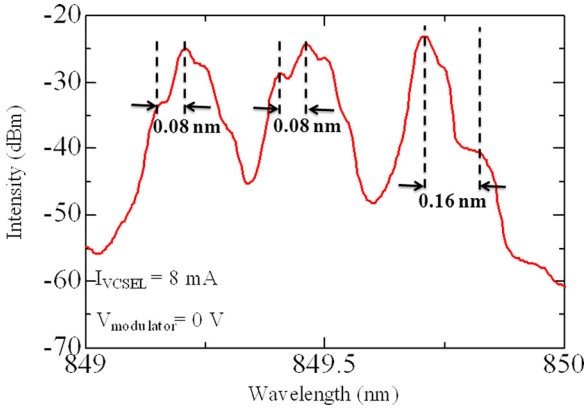

FIG. 4. Measured emission spectrum with the applied modulator voltage of 0 V.

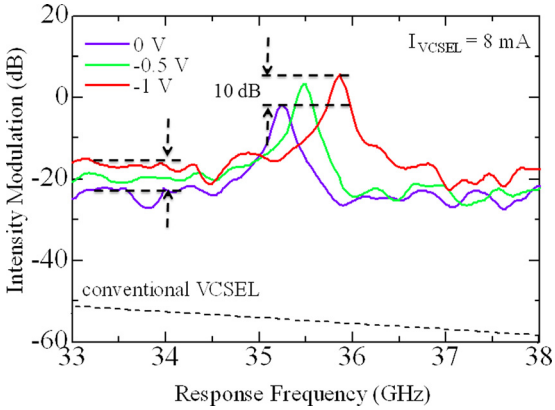

FIG. 6. Measured small-signal modulation response of the modulator integrated VCSEL with different reverse bias voltages of 0, 0.5, and 1 V with a VCSEL current of 8 mA.

could be increased by improving the coupling strength between the VCSEL and the modulator. Figure 4 shows the emission spectrum of the modulator output at an applied voltage of 0 V. The neighboring mode spacing is 0.08 and 0.16 nm, which is corresponding to 33 and 66 GHz in frequencies, respectively.

We measured the small signal frequency response by applying a RF signal in the modulator with a direct current (DC) reverse bias voltage. The VCSEL is pumped by a fixed DC current of 8 mA. Output light is captured by a photodetector (PD) with a 3-dB bandwidth of over 25 GHz through a multi-mode fiber. The measured small signal response (20 log x) is shown in Fig. 5. The small signal response of a conventional 850 nm VCSEL with an oxide aperture diameter of 8 μm, which was fabricated from the same wafer, is also shown for the comparison. The small signal response of the modulator-integrated device shows a large enhancement of over 55 dB in the modulation amplitude at a frequency beyond 35 GHz. The resonance frequency is in good agreement with the mode spacing for one of the sub-modes observed in Fig. 4. Also, we confirmed that the modulation efficiency, which is the modulation amplitude divided by the input RF amplitude, is only 3–4 dB lower than that of the directly modulated conventional VCSEL; thanks to the resonant type modulator. We see by increasing the reverse bias voltage from 0 V to 1 V that the peak intensity is enhanced by more 10 dB as shown in Fig. 6. This could be because the parasitic capacitance of the modulator section is reduced with increasing the bias voltage. Also, the resonance frequency is red-shifted with increasing the bias voltage, which could be due to the electro-refractive index change associated with the electro-absorption.

We calculated the small-signal modulation response of the modulator integrated VCSEL using a Fabry-Perot etalon model[31] with an electro-absorption. Figure 7 shows the calculated small signal response with a modulator length of 25 μm and a group index of 150. The small signal response of a conventional 850 nm VCSEL with a current density of 30 kA/cm^2 is also shown for the comparison. We assumed that the photon lifetime in the resonant cavity for the modulator is 0.5 psec and the 6-dB bandwidth limited by the parasitic capacitance is 26 GHz, which is estimated by fitting with the measured result shown in Fig. 5.[31] The resonant frequency and the enhancement in the modulation amplitude are almost in agreement with the experiment. It is noted that the second and third peaks at 68 GHz and 100 GHz appear with an amplitude enhancement of over 50 dB. In the experiment, we are not able to see the second peak because of the

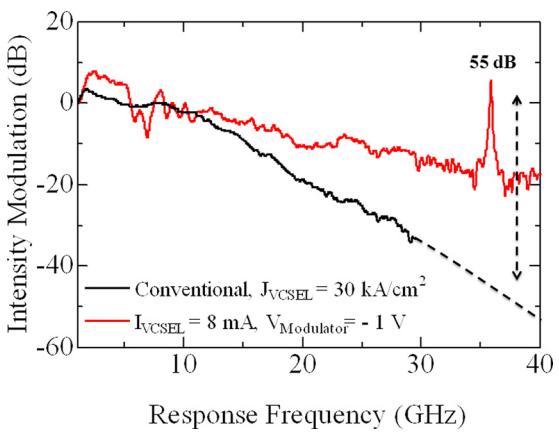

FIG. 5. Measured small-signal modulation response of the modulator integrated VCSEL with a reverse bias voltages of 1 V with a VCSEL current of 8 mA. The result of a conventional directly modulated VCSEL is also shown for comparison.

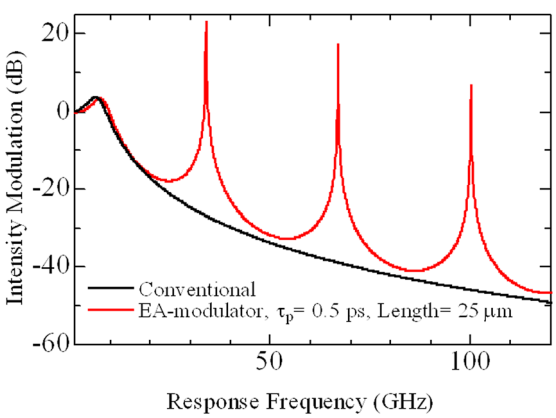

FIG. 7. Calculated small signal response of the slow-light resonant modulator. We assumed that the photon lifetime in the resonant cavity for the modulator is 0.5 ps and the 6-dB bandwidth limited by the parasitic capacitance is 26 GHz.

limited bandwidth of the photo-detector used in the experiment.

In conclusion, we demonstrated an ultra-compact (25 μm long) electro-absorption modulator laterally integrated with an 850 nm VCSEL incorporating a taper widening oxide aperture. The small signal response of the fabricated device shows a large enhancement of over 55 dB in the modulation amplitude at a frequency beyond 35 GHz. The resonance frequency could be tuned within 0.5 GHz by changing the reverse-bias voltage. We also calculated the small signal response by using a Fabry-Perot resonant modulator model. We expect a resonant modulation at a higher frequency of 100 GHz. The resonantly improved modulation characteristics play a significant key role for high efficient narrow-band modulation in the millimeter wave range over 35 GHz far beyond the intrinsic modulation bandwidth of VCSELs. Our ultra-compact modulator integrated VCSEL can boost the modulation speed far beyond the direct modulation for use in the next-generation computing and communication networks.

This work was supported by Grant-in-Aid for Scientific Research (S) from the Ministry of Education, Culture, Sports, Science and Technology of Japan (#22226008). This project was also funded by the deanship of Scientific Research (DSR), King Abdulaziz University, under Grant No. 20-130-35-RG. The authors, therefore, acknowledge with thanks DSR technical and financial support of KAU. The authors also would like to thank Dr. A. Matsutani for his support in dry etching processes.

[1]S. Kajiya, K. Ksukamoto, and S. Komaki, IEICE Trans. Electron. **E79-C**, 496 (1996).
[2]B. J. Koshy and P. M. Shankar, IEEE Trans. Veh. Technol. **48**, 847 (1999).
[3]J. Wells, IEEE Microwave Magn. **10**, 104 (2009).
[4]B. Razavi, IEEE Spectrum **45**, 46 (2008).
[5]C. Park and T. S. Rappaport, IEEE Wireless Commun. **14**, 70 (2007).
[6]L. A. Glasser, IEEE J. Quantum Electron. **16**, 525 (1980).
[7]K. Y. Lau and A. Yariv, Appl. Phys. Lett. **46**, 326 (1985).
[8]K. Y. Lau, Appl. Phys. Lett. **52**, 2214 (1988).
[9]R. Nagarajan, S. Levy, A. Mar, and J. E. Bowers, IEEE Photonics. Technol. Lett. **5**, 4 (1993).
[10]R. S. Tucker, U. Koren, G. Raybon, C. A. Burrus, B. I. Miller, T. L. Koch, and G. Eisenstein, Electron. Lett. **25**, 621 (1989).
[11]W. Kaiser, L. Bach, J. P. Reithmaier, and A. Forchel, IEEE Photonics Technol. Lett. **16**, 1997 (2004).
[12]K. Iga, Jpn. J. Appl. Phys., Part 1 **47**, 1 (2008).
[13]F. Koyama, IEEE/OSA J. Lightwave Technol. **24**, 4502. (2006).
[14]J. W. Scott, B. J. Thibeault, C. J. Mahon, L. A. Coldren, and F. H. Peters, Appl. Phys. Lett. **65**, 1483 (1994).
[15]A. Mutig, S. A. Blokhin, A. M. Nadtochiy, G. Fiol, J. A. Lott, V. A. Shchukin, N. N. Ledentsov, and D. Bimberg, Appl. Phys. Lett. **95**, 131101 (2009).
[16]N. Suzuki, T. Anan, H. Hatakeyama, K. Fukatsu, K. Yshiki, K. Tokutome, T. Akagawa, and M. Tsuji, IEICE Trans. Electron. **E92-C**, 942 (2009).
[17]P. Westbergh, R. Safaisini, E. Haglund, B. Kogel, J. S. Gustavsson, A. Larsson, M. Geen, R. Lawrence, and A. Joel, Electron. Lett. **48**, 1145 (2012).
[18]A. Larsson, IEEE J. Sel. Top. Quantum Electron. **17**, 1552 (2011).
[19]X. Zhao, Y. Zhou, C. J. Chang-Hasnain, W. Hofmann, and M. C. Amann, Opt. Express **14**, 10500 (2006).
[20]L. Chrostowski, X. Zhao, and C. J. Chang-Hasnain, IEEE Trans. Microwave Theory Tech. **54**, 788 (2006).
[21]C. Chen and K. D. Choquette, IEEE J. Lightwave Technol. **28**, 1003 (2010).
[22]T. D. Germann, W. Hofmann, A. M. Nadtochiy, J. H. Schulze, A. Mutig, A. Strittmatter, and D. Bimberg, Opt. Express **20**, 5099 (2012).
[23]C. Z. Ning and P. Goorjian, J. Appl. Phys. **90**, 497 (2001).
[24]C. Z. Ning, Opt. Lett. **27**, 912 (2002).
[25]R. Gordon, A. P. Heberle, and J. R. A. Cleaver, Appl. Phys. Lett. **81**, 4523 (2002).
[26]H. Dalir and F. Koyama, Appl. Phys. Lett. **103**, 091109 (2013).
[27]H. Dalir and F. Koyama, Appl. Phys. Express **7**, 022102 (2014).
[28]H. Dalir and F. Koyama, Electronics Lett. **50**, 823 (2014).
[29]H. Dalir, Y. Takahashi, and F. Koyama, Electron. Lett. **50**, 101 (2014).
[30]X. Gu, S. Shimizu, T. Shimada, A. Matsutani, and F. Koyama, Appl. Phys. Lett. **102**, 031118 (2013).
[31]E. L. Gordon and J. D. Rigden, Bell Syst. Tech. J. **42**, 155 (1963).